

Article

A Methodological Framework for Structural Reliability Assessment of Marine Structural Elements

Vaso Mantzakopoulou and Konstantinos Anyfantis * 

Ship-Hull Structural Health Monitoring (S-H SHM) Group, School of Naval Architecture and Marine Engineering, National Technical University of Athens, 9 Heroon Polytechniou Av., 15780 Zografou, Greece; vasomantzakopoulou@gmail.com

* Correspondence: kanyf@naval.ntua.gr; Tel.: +30-210-772-1325

Abstract: The aim of this paper is to provide a robust framework to assist researchers in deciding which methods to use, depending on the problem at hand, in order to estimate the probability of failure of marine structural parts that are subjected to variable loads (both hull-girder and local pressure loads) that exhibit uncertainties in their material properties and that involve fabrication-related uncertainties. The limitations of analytical approaches both in deterministic mathematical modeling (strength formulas) and probabilistic estimation will be provided, and respective computational tools will be demonstrated (FEA and Monte Carlo simulation). The approach is showcased in flat and bow-defected rectangular plates through analytical and numerical approaches.

Keywords: structural reliability analysis; stiffened panel; marine structures; probabilistic modeling; probability of failure



Citation: Mantzakopoulou, V.; Anyfantis, K. A Methodological Framework for Structural Reliability Assessment of Marine Structural Elements. *J. Mar. Sci. Eng.* **2023**, *11*, 2099. <https://doi.org/10.3390/jmse11112099>

Academic Editors: Mahmoud Chizari and Kazem Reza Kashyadeh

Received: 28 September 2023

Revised: 24 October 2023

Accepted: 25 October 2023

Published: 1 November 2023



Copyright: © 2023 by the authors. Licensee MDPI, Basel, Switzerland. This article is an open access article distributed under the terms and conditions of the Creative Commons Attribution (CC BY) license (<https://creativecommons.org/licenses/by/4.0/>).

1. Introduction

Ship hulls involve complex structural arrangements that are designed with the mandate to ensure the safety of the system for target reliability levels and for a specified time period. Their structural design involves different types of uncertainties and variabilities that are encountered both in terms of capacity (i.e., uncertainties in material properties, manufacturing processes and geometry) and in terms of the applied loads.

Traditionally, to account for these uncertainties and to meet the safety requirements at the design stage, designers utilize the so-called global safety factor, which has turned out to be conservative in many cases, since all the uncertainties are summarized in one single value. During recent decades, a transition has been taking place toward a more probability-based design method in order to quantify the uncertainties in a more rational manner, using probabilistic models as performed, for example, in [1–4]. This design method allows the use of partial safety factors (PSFs), which are defined in accordance with the regulatory framework and reflect the uncertainties in each of the variables. For instance, one may consult the Common Structural Rules (CSRs) [5] that are designated for bulk carriers and tankers. The most common format is the use of load-amplification factors and resistance-reduction factors. PSFs are determined by a target safety level, which is defined following reliability analysis of the structure or its components, and the design method is the so-called Load and Resistance Factor Design (LRFD) format. This approach has been applied for tankers [6], stiffened panels and grillages of ship structures [7,8] and unstiffened panels [9,10].

The structural reliability assessment of a ship structure as a whole or its individual assemblies (unstiffened or stiffened plates, double-bottom structure, etc.) performed utilizing reliability-based methods (e.g., Monte Carlo statistical simulation method, First-Order Reliability Method) has been attracting growing attention as it provides a rational framework for uncertainty quantification. This is, first of all, because of the need to know the reliability level of a system in order to avoid the risks brought by severe sea conditions

and emergencies and, secondly, because reliability analysis methods can be used as tools for safer and more robust engineering designs. Many studies [11–13] have proven the latter statement, with Mansour [14] being the first to conduct a reliability analysis of a hull structure. Additionally, the risk of failure in the design is comprehensively quantified and, as such, structural optimization may be performed in order to achieve weight savings. Structural reliability analysis (SRA) is concerned, apart from the calculation of PSFs, with the estimation and prediction of the probability of limit-state violation for an engineered system at any stage during its life. The violation of predefined limit states or of the so-called limit-state function (LSF) is considered to be a structural failure and lies at the heart of any reliability problem. Some possible forms of failure include collapse of the entire structure or its subcomponents, major cracking or excessive deflection.

In fact, SRA is an effective tool not only for safer engineering design but also for risk-based design, which is becoming an accepted design process for most ship types, providing a rational basis for making decisions on their design, operation and regulation. Risk in general can be defined as the potential of losses as a result of system failure and depends on the probability of failure and the degree of consequences arising from it. In [15], the relationship between risk evaluation and structural reliability was introduced, and then the evolution of structural reliability applied to ship structures was reviewed. The authors presented the limit-state function of a damaged ship with consideration of the special situations after collision and grounding, and they obtained the failure probabilities of the damaged ship based on the Monte Carlo simulation technique. In the context of risk-based design, the authors in [16] performed an SRA of an Aframax double-hull oil tanker using a proposed approach that captured, in a rational way, the complex interaction of different pertinent values influencing the safety of a damaged ship structure. The safety levels of the intact and the damaged ships indicated by the so-called reliability index was determined by employing the First-Order Reliability Method (FORM). The importance of conducting a structural reliability analysis was outlined, since its result, i.e., the probability of failure, is a vital part of the process of risk assessment and defines a target safety level.

Reliability-based methods have been demonstrated to be appropriate tools for assessing the level of safety or the probability of failure of ship structures and their components. This approach can lead to improvements in design. In paper [17], a hull-girder reliability assessment was performed using a Monte Carlo-based simulation method. Hull-girder reliability in an intact condition with several load combinations in the case of an oil tanker and a bulk carrier was investigated in [18]. The MC simulation method was performed; hence, the failure probability of still-water and wave-induced bending moments was obtained and discussed. The authors in [19] described reliability analysis carried out for two oil-tanker ships, demonstrating the feasibility and usefulness of reliability-based approaches in the development of ship longitudinal-strength requirements. FORM was utilized to solve the reliability problem and obtain the probabilities of failure in different load conditions. Paper [18] focuses on hull-girder reliability analysis via MC simulation and sensitivity analysis of an oil tanker and a bulk carrier in intact condition.

The classical SRA of intact ship hulls is also extended to the case of ships with damage or completely collapsed ships in order to determine the options for recovery or to result in a possible review of design rules correspondingly. The MOL Comfort accident in 2007 was investigated using a reliability-based method, which estimated the possibility of occurrence of the fracture, i.e., probability of failure, suggesting a review of the relevant classification rules [20]. In addition, the Prestige accident in 2002 showed the importance of a reliable assessment of damaged vessels' longitudinal strength in real emergency situations and time pressure. The authors in [21] studied the residual strength and the reliability of tankers following damage using a reliability-based method. In [22], the probabilistic characteristics of the hull-girder safety level of a Suezmax tanker were assessed. The hull-girder probability of failure was estimated using the FORM, considering the ultimate collapse of the mid-ship section. A time-variant reliability analysis of a bulk carrier in damage conditions after a collision event was performed by MC simulation in [23].

Concerning the problem of assessing the structural reliability of a structure or one of its components, a methodological approach needs to be adopted. This approach should focus on formulating the limit-state equations, which are essential for conducting reliability analysis. The quantification of the uncertainties involved in the description of the load and the structural capacity in a rational manner through probabilistic models, i.e., random variables, is also a vital part of the procedure. The complexity of the problem and the number of input variables that are considered to be random determine whether the limit-state equations can have an explicit or an implicit expression.

Having studied the literature body that concerns structural reliability problems, it can be concluded that a comprehensive guideline for solving the reliability problem has not yet been proposed. This paper fits in this gap of the literature since it presents a methodological framework that applies to the estimation of the probability of violating a certain limit-state equation. It is considered that the problem involves variability in the uncertain loads, including both hull-girder and local pressure loads and uncertainties in the material properties and geometrical parameters, e.g., fabrication-related uncertainties and geometrical tolerances. In simple words, the aim of this paper is to provide a robust framework that assists the analyst to decide upon which methods to use, depending on the problem at hand, so as to estimate the probability of failure of marine structural parts. The presented framework is showcased in a rather simple but important case that is encountered during the design of ship structures: that is, an unstiffened plate which is subjected to local and global loads. The approach will be demonstrated in both a flat and a bow-defected rectangular plate through analytical and numerical approaches. The unstiffened plate is a good and typical benchmark case. That is because there are analytical methods to solve the problem when dealing with a flat plate, but once an initial imperfection is added to it, utilizing numerical methods for the solution is inescapable.

This paper is structured as follows: In Section 2, the fundamentals of structural reliability are briefly outlined. The proposed SRA framework and its ingredients, i.e., the proposed methods for solving the reliability problem, are also detailed. Section 3 deals with the definition of the problem that the framework is going to be showcased in. One part of the presented framework is demonstrated in a flat plate in Section 4, and the other part of the framework is demonstrated in a curved plate in Section 5.

2. Reliability Analysis Framework

2.1. Fundamentals of Structural Reliability

The main goal of an SRA of a ship's structural component is to evaluate its corresponding probability of failure, p_f , or its reliability, R_o [24,25]. These two probabilities sum up to unity,

$$p_f + R_o = 1 \Rightarrow p_f = 1 - R_o \quad (1)$$

since they are connected with two mutually exclusive complementary events. Defining the acting loads or the load effects as S and the corresponding resistance as R , the safety margin or the LSF, G , may be defined as

$$G = g(r, s) = R - S \quad (2)$$

The LSF can mathematically articulate the definition of failure. Since SRA is a probability-based analysis, R and S are considered to be random variables, and as such, they are associated with a statistical structure that may be denoted by $f_R(r)$ and $f_S(s)$, respectively. These correspond to separate probability density functions (PDFs). Consequently, G is also a random variable with a corresponding PDF, which is denoted as $f_G(g)$. Structural failure can be defined as an event where the load effect is larger than the resistance

$$G = R - S \leq 0 \text{ or } G \leq 0 \quad (3)$$

And thus, the probability of failure for a fundamental reliability problem takes the form:

$$p_f = P(R \leq S) = P(R - S \leq 0) = P(G \leq 0) = \int_{-\infty}^0 f_G(g) dg \quad (4)$$

A rather convenient form of the limit-state function that describes a common family of structural reliability problems may be written as:

$$G(R, \mathbf{X}) = R - S(\mathbf{X}) \quad (5)$$

Magnitude \mathbf{X} corresponds to the random vector that contains the basic random variables that control the load effect and may be either deterministically or probabilistically quantified. For example, variability in local or global wave-induced loads (pressure of hull-girder resultants) influences the stress state at any point of the hull. Variability in the geometric tolerances and material properties has also an immediate effect on the stress field. All these quantities may well be considered as basic random variables that influence the load effect of interest, which in turn may be statistically correlated or uncorrelated. Function $S(\cdot)$ can be considered to be either an analytical or a numerical predictive model that provides a mapping between a realized random vector and the load effect. Modeling the resistance of the structural component as a random variable accounts for the uncertainty in the geometric and material properties of the structural element. In many practical applications, the resistance of the structure may be significantly affected by the variability of the input values, and that correlation is expressed by the correlation coefficient. However, in the present study, it was considered that the random variables which affect the load effect (e.g., the load, structure's dimensions) are statistically independent of the resistance of the structure (i.e., steel's yield stress). The objective following the formulation of the LSF is to estimate the probability of failure of the structural part, using the proper reliability method in terms of accuracy and time efficiency.

The focus of the present demonstrative study is on the linear elastic structural behavior of a representative marine geometry; hence, the resistance (R) of the demonstrated structure was considered to be the yield stress (σ_y) of the material, and the load effect (S) was considered to be the maximum equivalent stress (i.e., Von Mises stress) occurring (σ_{VM}). In other applications, a different limit-state design can be studied, such as buckling or the ultimate limit state of ship structures, as seen in [26–29]. Concerning the former, the yield stress of the material is supposed to be the resistance (R), while the ultimate compressive strength (σ_u) of the structure is supposed to be the load effect (S). However, when studying an ultimate limit state, R is considered to be a hull girder's ultimate bending capacity (M_u), and S is considered to be the applied vertical bending moment (M). In all the aforementioned limit-state design studies, the limit-state function is formulated according to Equation (2).

2.2. Proposed SRA Framework and Its Ingredients

The specifications and the nature of the problem determine the method that is going to be employed in order to estimate the failure probability. The entire framework, illustrated in Figure 1, is designed in order to help the researcher decide which reliability method to use depending on the problem in order to estimate the probability of failure of a structural component. One central question that drives the SRA framework is whether there is an analytical mathematical expression for the mapping function $S(\cdot)$. If the answer is positive, then a separate path between a linear S function with respect to the RVs and a non-linear one is defined. If S is a linear function, there are three ways to solve the problem. Generally, it should be noted that the random variables can correspond to different types of probability distributions. In addition to other types of parametric probability distributions often published in the literature, random variables can be expressed in the case of a large amount of measured data (e.g., using monitoring) utilizing histograms (empirical non-parametric probability distribution). In the present study, if the random variables follow a normal ($\mathbf{X} \sim N$) or a lognormal ($\mathbf{X} \sim LN$) distribution and the distribution of the random

variable R is normal ($R \sim N$) or lognormal ($R \sim LN$), respectively, then this is the only case where an analytical method can be applied to estimate p_f . Another approach is to estimate the statistical behavior of S , using realizations from a Monte Carlo simulation (MCS). If S is shown to follow a normal distribution, then an approximate method can be employed if and only if R is normally distributed or assumed to be. A numerical method, that is the Monte Carlo (MC) method for estimating the probability of failure, can also be employed irrespective of the statistical behavior of the input random variables. The approximate and the numerical method mentioned above can also be used in the case where the function of S is non-linear. Another approach for this case is to linearize the function S and then apply an approximate method, which is applicable only if the variable R is considered to follow a normal distribution.

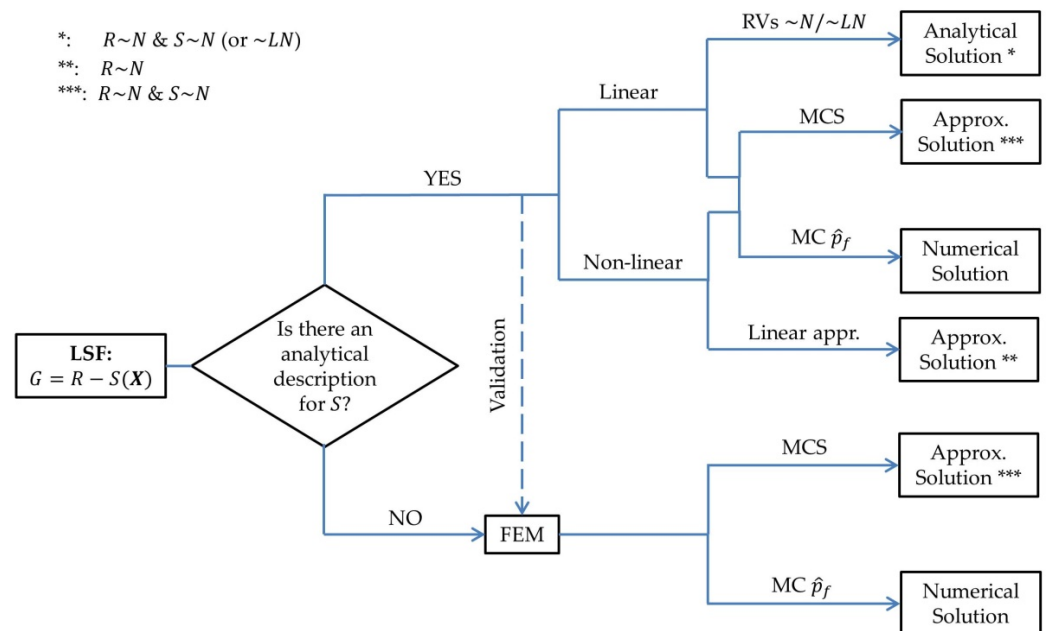


Figure 1. Framework of deciding which reliability method to use depending on the problem.

In the case where S cannot be analytically expressed, then a numerical procedure, such as the Finite Element Method (FEM), needs to be applied in order to obtain realizations of the response of the structure on the applied loads. An MC simulation may be employed directly for the estimation of the probability of failure or may be employed for estimating the distribution of S and then solving the reliability problem analytically if the conditions allow (normality or lognormality in both S and R hold). The aforementioned procedure is of course applicable for the case where mathematical expression for S does exist, but it is usually used for benchmarking and validation purposes.

2.2.1. Cornell’s Reliability Index

In case the mapping function, S , is a linear function of the basic variables (X) and if the basic variables are normally distributed, S is also normally distributed. The mean and the variance of the load effect, S , may be obtained from operations between the moments of the basic random vector with information provided in the Appendix A. The mathematical definition of failure is taken in accordance with Equation (3). Taking into account that R is also normal, then the reliability index can be defined according to Cornell as follows:

$$\beta = \frac{\mu_G}{\sigma_G} = \frac{\mu_R - \mu_S}{\sqrt{\sigma_R^2 + \sigma_S^2 + 2\rho_{R,S} \sigma_R \sigma_S}} \tag{6}$$

where $\mu_{i=R,G,R,S}$ is the mean value of the denoted RV, $\sigma_{i=G,R,S}$ the standard deviation of it and $\rho_{R,S}$ is the correlation coefficient between R and S . More information is provided in Appendix A.

That is, β is the reciprocal of the coefficient of variation of G . The concept of β is illustrated in Figure 2 which shows the PDF of G for the fundamental case of a two-variable problem. The safety is defined by the event $G > 0$, and consequently, failure is defined by $G < 0$. The reliability index may be thought of as the distance from the origin ($G = 0$) to the mean μ_G measured in standard deviation units. As such, β is a measure of the probability that G will be less than zero.

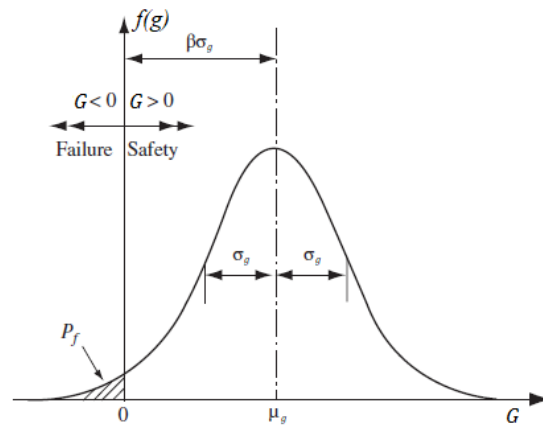


Figure 2. Concept of reliability index, $G = R - S$, R and S normal and independent.

In case the basic variables are lognormal and independent, then the logarithm of S , i.e., $\ln S$, is normally distributed, since the sum of the logarithms of the random variables is normal distributed. The mean and the standard deviation of the variable $\ln S$ are provided in Appendix A. Taking into account that R is also considered to be lognormal distributed, the alternative formulation for failure is taken. That is, for failure

$$\left(\frac{R}{S}\right) < 1 \text{ or } \ln\left(\frac{R}{S}\right) < 0 \tag{7}$$

The reliability index can be defined, using the small variance approximations, as

$$\mu_G = E\left[\ln\left(\frac{R}{S}\right)\right] \approx \ln\left(\frac{\mu_R}{\mu_S}\right) \tag{8}$$

$$\sigma_G^2 = \text{Var}\left[\ln\left(\frac{R}{S}\right)\right] \approx \sigma_{\ln R}^2 + \sigma_{\ln S}^2 + 2\rho_{\ln R, \ln S} \sigma_{\ln R} \sigma_{\ln S} \tag{9}$$

$$\beta = \frac{\ln\left(\frac{\mu_R}{\mu_S}\right)}{\sqrt{\sigma_{\ln R}^2 + \sigma_{\ln S}^2 + 2\rho_{\ln R, \ln S} \sigma_{\ln R} \sigma_{\ln S}}} \tag{10}$$

where $\rho_{\ln R, \ln S}$ is the correlation coefficient between the RVs $\ln R$ and $\ln S$.

The probability of failure, for both cases, is related to the reliability index as follows:

$$p_f = \Phi(-\beta) \tag{11}$$

where $\Phi(\cdot)$ is the cumulative distribution function for the standard normal distribution.

It should be noted that the mapping function, S , has been assumed to be a linear combination of the basic variables so far. However, this may not be true most of the time in practice. If the function for S is non-linear, then the Mean Value First-Order Second-Moment method (MVFOSM) can be applied. The MVFOSM method does not consider the distributions of the random variables and directly carries out the first-order Taylor

expansion of S at the mean. The approximate values of μ_S and σ_S are obtained by Equations (A6) and (A7), respectively. More information is provided in Appendix A. Following the linearization of the function S , an approximate solution can be implemented if and only if R is also considered to be normal distributed. That is, the reliability index and the probability of failure can be estimated using Equations (6) and (11), respectively.

2.2.2. Monte Carlo Simulation (MCS) Method

It should be noted that the accuracy and the feasibility of the methods described in Section 2.2.1 decrease with increasing non-linearity for the response of the structure (S) and the number of non-normal random variables. In such cases, the failure probability may be estimated by simulation methods, such as the Monte Carlo simulation method. The MC method can be used either for a direct estimation of the probability of failure irrespective of the distribution of the random variables or for the estimation of the statistical behavior of the variable S , which may lead afterwards to an approximate solution of the problem under certain conditions.

Concerning the MC probability of failure estimator (\hat{p}_f), the technique involves “sampling” at “random” to simulate artificially a large number of experiments and to observe the result. In this case of analysis for structural reliability, this means, in the simplest approach, generating (or simulating) a large number of realizations of the basic random variables X (i.e., $x_j, j = 1, 2, \dots, N$) and of the variable R (i.e., $r_j, j = 1, 2, \dots, N$). The realizations are then fed forward to Equation (5), and for each of the outcomes g_j , it is checked repetitively whether or not the limit-state function taken in (x_j, r_j) is positive. All the simulations, for which this is not the case, are considered as failure and are counted (n_f). After n simulations, an unbiased estimation of the failure probability p_f may be estimated through the following:

$$\hat{p}_f = \frac{n_f}{n} \tag{12}$$

which then may be considered a sample expected value of the probability of failure. Obviously, the number of N trials required is related to the desired accuracy of \hat{p}_f . In fact, for $N \rightarrow \infty$, the estimate of the probability of failure becomes exact. However, simulations are often costly in computation time, and the uncertainty of the estimate is thus of interest.

The MC method is also used for Uncertainty Quantification (UQ), aiming to provide quantifiable estimations on the variability (uncertainty) associated with the Quantities of Interest (QoIs). As already mentioned in Section 2.2, a mapping between X and Y can be assigned to the computational model, S , which receives a specific realization of X and returns the corresponding output $y = S(x)$. Sampling a sufficiently large amount of realizations from the random variables $\{x_{j=1}, x_{j=2}, \dots, x_{j=n}, j = 1, 2, \dots, n\}$, which will be then fed forward to the computational model $S(x)$, outcome instances are produced, i.e., $\{y_{j=1}, y_{j=2}, \dots, y_{j=n}, j = 1, 2, \dots, n\}$. The latter are collected and statistically analyzed. It has been shown that the method can achieve a complete description of the statistical behavior of the output Y if a large number of random samples are simulated. The QoIs are considered to be f_y, μ and σ^2 with the goal of providing statistical inferences for them.

Sample statistics may be used as point estimates, since the MC estimators are unbiased in the sense that they converge to the true, yet unknown, value of the QoI: that is, the sample mean value of Y and the variance, which along with the underlying PDF f_Y may fully characterize the statistical behavior of the variable S . The sample mean (average), \bar{y}_n , is a point estimator for the expected value of Y :

$$\mu = \bar{Y}_n = \frac{1}{n} \sum_{i=1}^n y_i \tag{13}$$

And the sample variance is the point estimator for the variance of Y :

$$\sigma^2 = s_n^2 = \frac{1}{n-1} \sum_{i=1}^n (y_i - \bar{y}_n)^2 \tag{14}$$

Following the procedure above, if S is concluded to be normal distributed, as the variable R is considered to be, an approximate solution can be implemented. That is, the reliability index and the probability of failure can be estimated using Equations (6) and (11) correspondingly, where μ_S is taken from Equation (13) and σ_S is taken from Equation (14).

3. Problem Definition

3.1. Problem Description

The plate considered as a case study in the present reliability assessment is an external bottom plate (unstiffened area between two successive floors and two successive stiffeners) from a typical tanker geometry. The plate has a length a of 3780 mm, a width b of 800 mm and a thickness t of 13 mm. The considered vessel has a mid-ship section modulus Z of 29.02 m³. The material of the plate was considered to be high tensile strength steel with a characteristic yield stress magnitude of 315 MPa. Figure 3a shows the mid-ship section of the fictional tanker, and Figure 3b shows a top view of the plate under consideration.

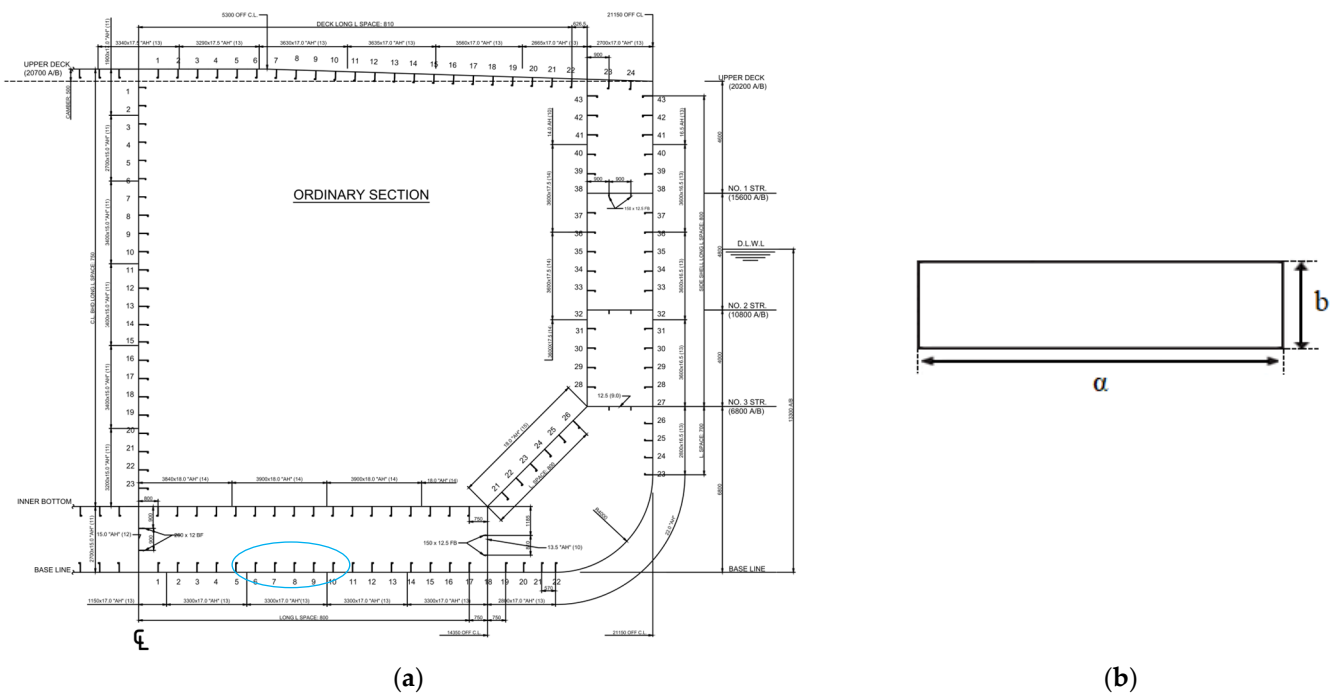


Figure 3. (a) Mid-ship section of the fictional tanker vessel, (b) 2D view of the plate under consideration.

Concerning the load effects acting on the plate, it was considered to be either the tertiary stresses resulting from a uniformly applied pressure on the surface of the plate or the combination of the primary stresses resulting from the hull girder bending and the tertiary stresses together. The pressure involves the hydrostatic pressure due to still waves, P_{sw} , with a design value of 0.133 MPa and the pressure due to waves, P_w , with a design value of 0.076 MPa. The bending moment involves the still water bending moment, M_{sw} , with a design value of 1873 MNm and the wave-induced bending moment, M_w , with a design value of 3827 MNm.

3.2. Stochastic Models of the Parameters of the Problem

The basic parameters of the problem under consideration concern the strength of the plate and the loads acting on it. As described in Section 2.2, the actual values of the variables related to the strength of the plate, such as the yield stress of the material, the plate thickness, etc., and to the loads acting on it, such as the hydrostatic pressure, primary stresses, etc., tend to behave in a random manner. Variations in strength, load and load effects greatly impact the reliability of a structural system. Therefore, in order to account for this variability in the variables, the latter need to be approached in a probabilistic manner,

i.e., as random variables. The research team in [30] compiled statistical information and data based on a literature review on both strength and load random variables for quantifying the probabilistic characteristics of these variables. The recommended distribution for the yield stress, R , of a high tensile steel with a design value of 315 MPa was the lognormal one with a mean equal to 342 and a COV of 0.089. The probabilistic characteristics of all the random variables considered in the problem are calculated in line with [30] and are shown in Table 1. The random variables were considered to be uncorrelated. Poisson’s ratio ν was assumed to be deterministic, and thus, a value of 0.3 was considered.

Table 1. Stochastic models of the parameters of the problem.

Variable	Distribution	Mean μ	COV
M_{sw} (MNm)	Normal	936.7	0.6
M_w (MNm)	Largest Extreme Value (Type I)	3827.10	0.15
P_{sw} (MPa)	Normal	0.067	0.15
P_w (MPa)	Largest Extreme Value (Type I)	0.076	0.15
b (m)	Normal	0.7936	0.028
t (m)	Lognormal	0.0137	0.044
Z (m ³)	Normal	30.18	0.05

It should be noticed that although R is lognormal distributed, it can be assumed to be normal distributed without introducing error to the estimation of the probability of failure, as Figure 4 depicts. Figure 4 shows the PDF of the lognormal distributed R and the PDF of a normal distributed random variable with a mean equal to 342 MPa and standard deviation equal to 30.4 MPa.

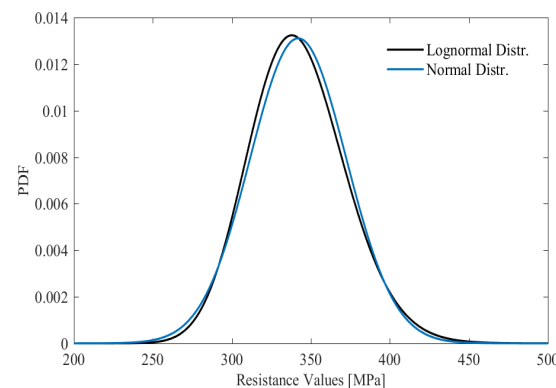


Figure 4. Probability density functions of the lognormal distributed R and of a normal distributed random variable with mean equal to 342 MPa and standard deviation equal to 30.4 MPa.

Concerning the bow deflected plate, the geometry and magnitude of the imperfection are stochastic per se, and as such, there are considered to be uncertain quantities, as proposed by the authors in [31]. More specifically, the initial geometric imperfection shape (W_o) of the plates can be represented by only one component of the Fourier series as follows:

$$W_o(x, y; W_{max}) = W_{max} \sin\left(\frac{\pi x}{a}\right) \sin\left(\frac{\pi y}{b}\right) \tag{15}$$

where a and b are the plate’s dimensions and W_{max} is the amplitude of the shape of the initial imperfection. The mean value of W_{max} was equal to 2.015 and the coefficient of variation (COV) was equal to 1.57, according to [31]. A visual representation of the underlying statistical structure of W_{max} is shown in Figure 5.

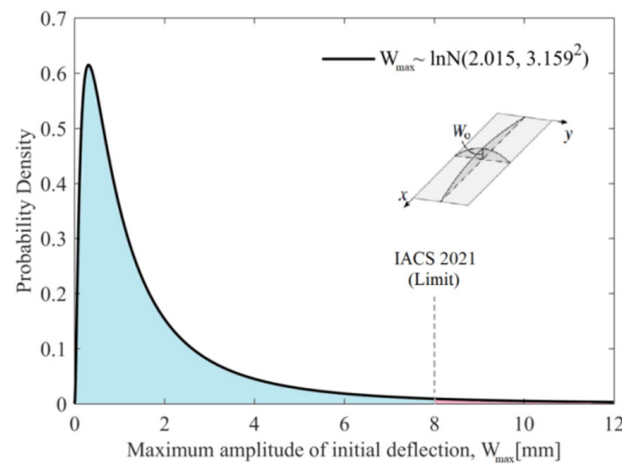


Figure 5. Probability density function plot of the maximum magnitude of the initial deflection W_0 .

It should be noted that the uncertainty of the geometric imperfection could be modeled in various ways. In paper [32], where the ultimate strength of stiffened panels of ships considering uncertainties in geometrical aspects was assessed, the initial geometric imperfection was imposed in the form of a column imperfection mode on the entire stiffened panel, a torsional imperfection mode on the stiffener and a local imperfection mode on the plate and flange. The authors in [4] introduced a newly proposed probabilistic-based imperfection model via the spectral representation method, while in paper [33], a comparison of the prevailing geometric imperfection models (e.g., hungry-horse mode, admiralty research establishment mode and critical buckling mode) and their influence on the ultimate compressive strength of ship grillages is completed.

4. Reliability Analysis of Flat Plates

Considering the framework proposed in Figure 1, Section 4 demonstrates the cases for which there is an analytical mathematical expression for the mapping function $S(\cdot)$. Case study 1 refers to the path where S is a linear function with respect to the RVs, whereas case study 2 refers to the path where S a non-linear one.

4.1. Case Study 1: Flat Plate Subjected to Tertiary Stresses

In case study 1, the plate is subjected only to hydrostatic pressure due to still water (P_{sw}), which is considered random along with the resistance of the plate R . The values of the thickness and width of the plate were the design ones. Concerning the constraints at the edges of the plate, a clamped plate, which is shown in Figure 6, was examined. The point where the maximum equivalent stress (or Von Mises stress) occurs is denoted as 1 in Figure 6.

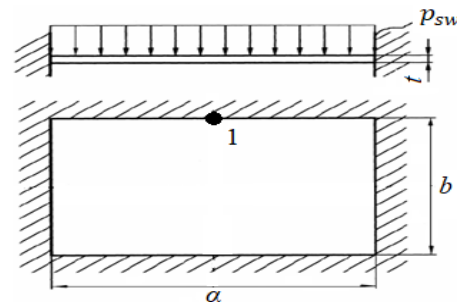


Figure 6. Clamped plate under p_{sw} .

The equivalent stress is a function of the random variable P_{sw} , as can be seen by Equation (16), which refers to point 1.

$$S_1 = \sqrt{\left[\frac{1}{2} \nu P_{sw} \left(\frac{b}{t} \right)^2 \right]^2 + \left[\frac{1}{2} P_{sw} \left(\frac{b}{t} \right)^2 \right]^2 - \left[\frac{1}{2} \nu P_{sw} \left(\frac{b}{t} \right)^2 \right] \left[\frac{1}{2} P_{sw} \left(\frac{b}{t} \right)^2 \right]} = 1.683 P_{sw} \tag{16}$$

Therefore, the LSF is formulated as follows:

$$\begin{aligned} G_1(P_{sw}, R) &= R - S_1(P_{sw}) \\ &= R - \sqrt{\left[\frac{1}{2} \nu P_{sw} \left(\frac{b}{t} \right)^2 \right]^2 + \left[\frac{1}{2} P_{sw} \left(\frac{b}{t} \right)^2 \right]^2 - \left[\frac{1}{2} \nu P_{sw} \left(\frac{b}{t} \right)^2 \right] \left[\frac{1}{2} P_{sw} \left(\frac{b}{t} \right)^2 \right]} \\ &= R - 1.683 P_{sw} \end{aligned} \tag{17}$$

Equation (16) indicates that S is a linear function of the RVs, i.e., P_{sw} . Therefore, the probability of failure can be estimated three different ways, if the conditions allow, as Figure 1 proposes: with the analytical method, with the approximate method that utilizes the MCS and with the numerical method that applies MC to estimate the probability of failure.

The analytical method, i.e., Cornell’s reliability index method (Equation (16)), resulted in a probability of failure of 2.13×10^{-11} , which was estimated according to Equation (11). Concerning the approximate method, it includes the utilization of the MC method in order to estimate the distribution of S and then solve the problem using Cornell’s reliability index if the conditions allow. In simple words, a sample of size 10^5 was generated from the normal distributed P_{sw} . Each sample was then fed forward to the load effect S , according to Equation (16). The sample statistics of S were estimated, and the histogram indicated that S follows a normal distribution. Therefore, Cornell’s reliability index could be calculated according to Equation (6), resulting in a p_f equal to 2.04×10^{-11} , which was estimated according to Equation (11). For the sake of applying the MCS directly for estimating the p_f , a sample of size at least 1.4×10^{11} was needed to be generated from R and S in order for the method to result in an indicative probability of failure, according to [34]. The size of these simulations was neither cost efficient nor achievable timewise.

4.2. Case Study 2: Flat Plate Subjected to Primary & Tertiary Stresses

In case study 2, the plate was subjected to both primary and tertiary stresses. More specifically, the tertiary stresses were a result of the combination of the hydrostatic pressure due to waves and the one due to still water, and the primary stresses were a result of the combination of the bending moment due to waves and the one due to still water. Concerning the constraints at the edges of the plate, a clamped plate, which is shown in Figure 7, was examined. The points where the maximum equivalent stress may occur are denoted as 1 and 2 in Figure 7.

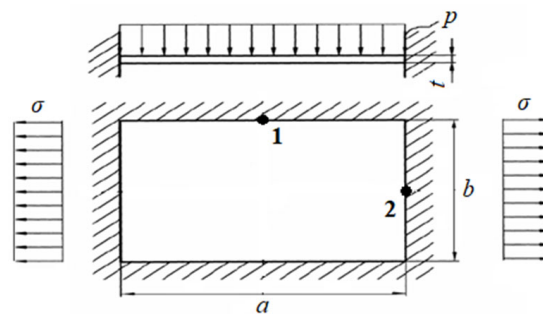


Figure 7. Clamped plate under primary and tertiary stresses.

Since it is not known a priori where the maximum equivalent stress is going to occur, the function of S was formulated for both point 1 and point 2 as follows:

$$S_1 = \sqrt{\left[\frac{1}{2} \nu P \left(\frac{b}{t} \right)^2 + \frac{M}{Z} \right]^2 + \left[\frac{1}{2} P \left(\frac{b}{t} \right)^2 \right]^2} - \left[\frac{1}{2} \nu P \left(\frac{b}{t} \right)^2 + \frac{M}{Z} \right] \left[\frac{1}{2} P \left(\frac{b}{t} \right)^2 \right] \quad (18)$$

$$S_2 = \sqrt{\left[0.34 P \left(\frac{b}{t} \right)^2 + \frac{M}{Z} \right]^2 + \left[0.34 \nu P \left(\frac{b}{t} \right)^2 \right]^2} - \left[0.34 P \left(\frac{b}{t} \right)^2 + \frac{M}{Z} \right] \left[0.34 \nu P \left(\frac{b}{t} \right)^2 \right] \quad (19)$$

All the variables that appear in Equations (18) and (19), apart from Poisson’s ratio, ν , are considered to be random. Concerning the limit-state function, it can be expressed according to Equation (5); Equation (20) refers to point 1 and Equation (21) refers to point 2:

$$G_1(t, b, P_{sw}, P_w, M_{sw}, M_w, Z, R) = R - S_1 \quad (20)$$

$$G_2(t, b, P_{sw}, P_w, M_{sw}, M_w, Z, R) = R - S_2 \quad (21)$$

Equations (18) and (19) indicate that S is not a linear function of the basic random variables. Therefore, the probability of failure can be estimated three different ways, if the conditions allow, as Figure 1 proposes: with the approximate method that includes the linearization of S , with the approximate method that utilizes the MCS and with the numerical method that applies MC to estimate the probability of failure.

Following the linearization of S_1 and S_2 , the mean value and the standard deviation of these RVs were estimated according to Equations (A9) and (A11), respectively. In order to evaluate the linearization that was made by Taylor’s series expansion, the function of the maximum Von Mises stress was plotted seven times for both points, and each time, one of the independent variables was taking values inside the interval $(-4\sigma + \mu, 4\sigma + \mu)$ (where σ is the standard deviation and μ is the mean of the variable), and the other variables were held constant using their mean values.

It can be concluded from Figure 8 that the linear approximation of the load, S , seems to be a good fit around the mean value for each of the curves. It should be noted that the mean value of the maximum equivalent stress that occurred at point 2 (=281.18 MPa) was higher than that which occurred at point 1 (=227.87 MPa), so the former was used to proceed with the estimation of the probability of failure. An approximate solution that utilizes Cornell’s reliability index, calculated by Equation (6), could be implemented, resulting in a probability of failure of 8.51×10^{-2} , according to Equation (11).

According to the Central Limit Theorem, it was expected that the distribution of S would be normal, following its linearization. However, the approximate method used in this case is a simplified method for linearizing a function, and it could introduce significant errors in the final result. More specifically, Figure 8 shows that for values around the mean value of each random variable, the linear approximation seems to be a good fit to the real function. However, when the values of the random variables come from the outliers of their distribution, the linear approximation deviates a lot from the real function. Therefore, significant errors may be introduced at increasing distances from the linearizing point by neglecting higher-order terms in Taylor’s series expansion. On top of that, the linearization point was chosen to be the mean value of the maximum Von Mises stress, which of course might not be the optimal choice.

The problem could also be solved utilizing the MC \hat{p}_f estimation method. In order to do so, a sample of size 10^5 was generated from each of the RVs. Each sample was then fed forward to Equations (20) and (21) while examining which value that resulted from them was higher. The probability of failure was estimated according to Equation (12) and was equal to 2.9×10^{-3} . Figure 9 shows that the MC mean estimator of the probability of failure converges to the true yet unknown probability of failure. The lower and the upper

bounds correspond to confidence intervals of 95% confidence level. It should be noted that a simulation with an increasing sample size up to 10^6 or 10^7 was not achievable timewise.

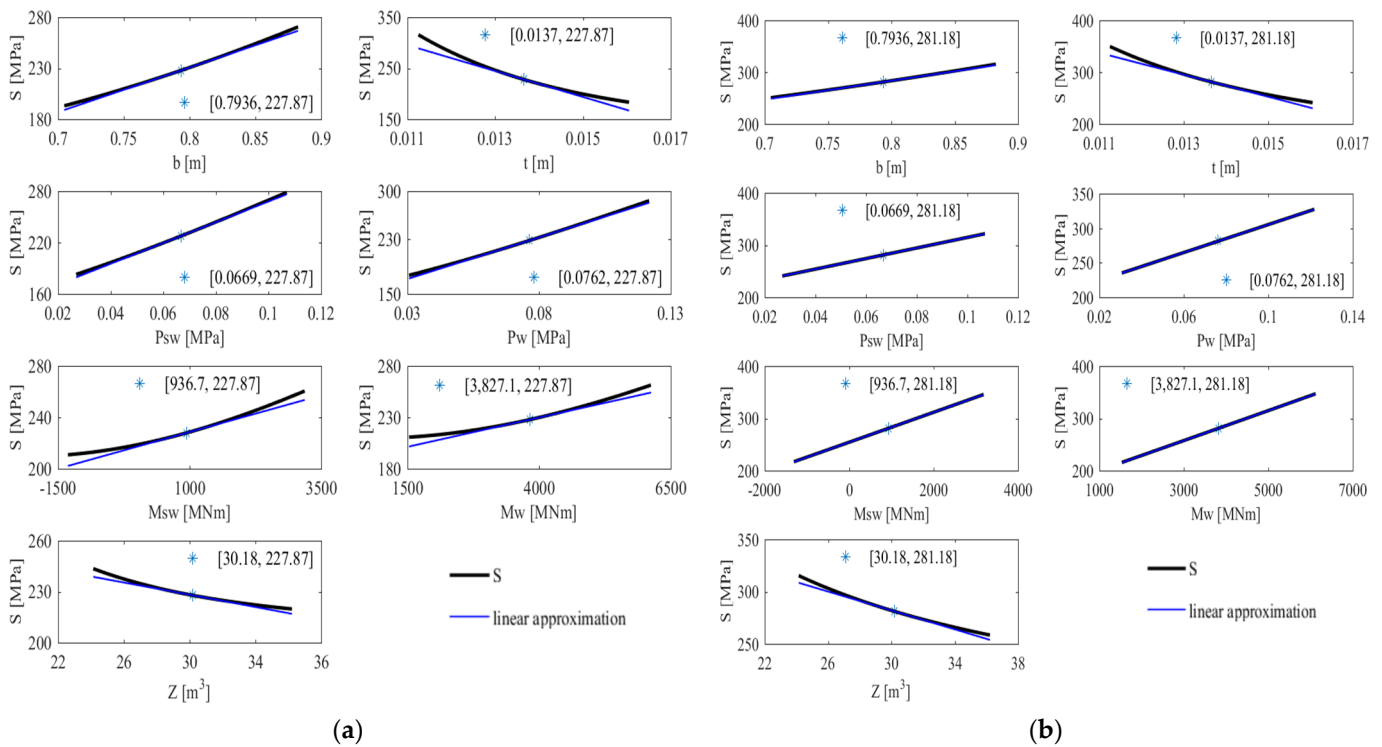


Figure 8. (a) Equivalent stress function plots with respect to each variable and the function's linear approximation (point 1); (b) equivalent stress function plots with respect to each variable and the function's linear approximation (point 2).

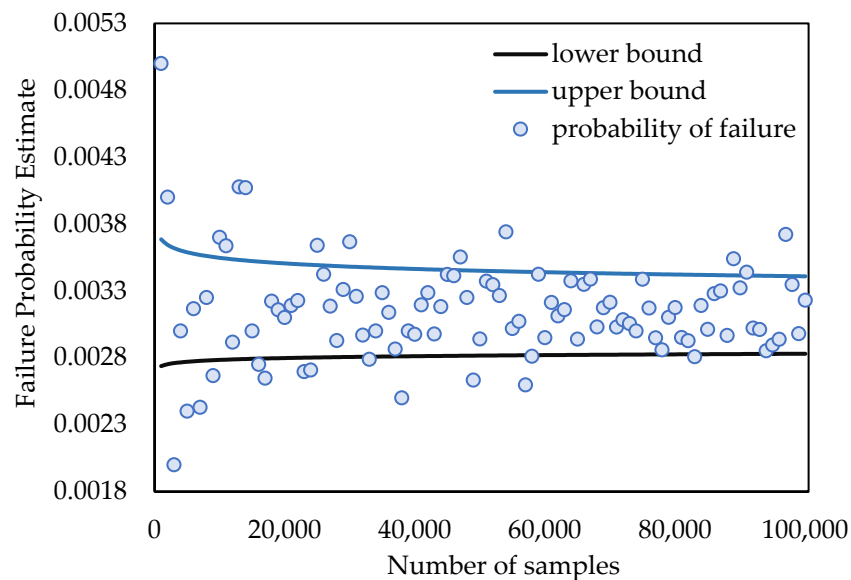


Figure 9. MC convergence graph—sample size up to 10^5 .

Concerning the approximate method, which includes the utilization of the MC method in order to estimate the distribution of S and then solve the problem using Cornell's reliability index, it could not be applied because the conditions did not allow it. More specifically, a sample of size 4×10^4 was drawn from each of the RVs from Equations (18) and (19), and the realizations were then fed forward to Equations (18) and (19), respectively. The instances of S_1 and S_2 were then collected and statistically analyzed. Since the number of the

samples that were simulated was large, the method could achieve a complete description of the statistical behavior of the output S_1 and S_2 . The moments of S_1 and S_2 that were estimated indicated that the mean value of the maximum equivalent stress is higher at point 2 (267 MPa) than that at point 1 (220 MPa). A convergence plot of the MC estimator of the maximum equivalent stress at point 2 was also constructed, as shown in Figure 10, for illustrative purposes. A histogram and a QQ plot were created out of the realizations of S_2 in order to examine whether the distribution of S_2 is normal, as shown in Figure 11.

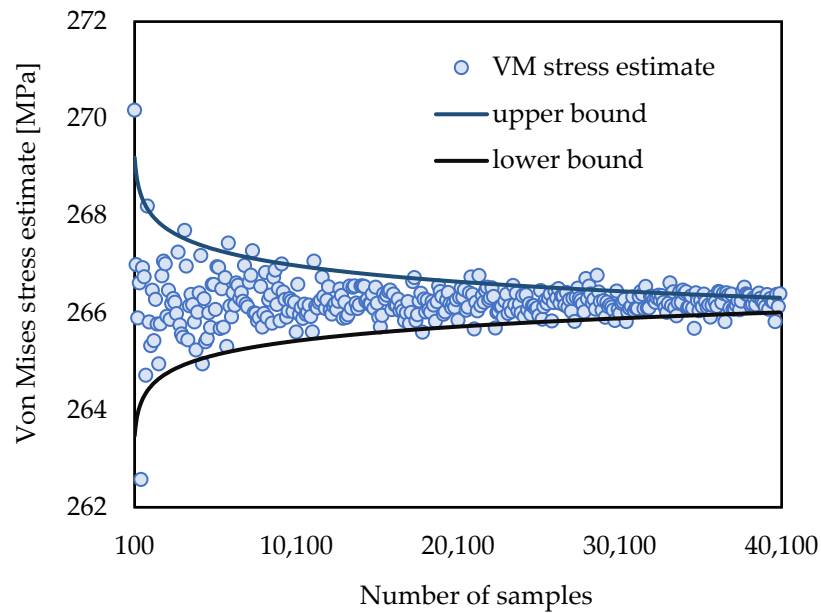


Figure 10. MC convergence plot of the equivalent stress at point 2 estimate.

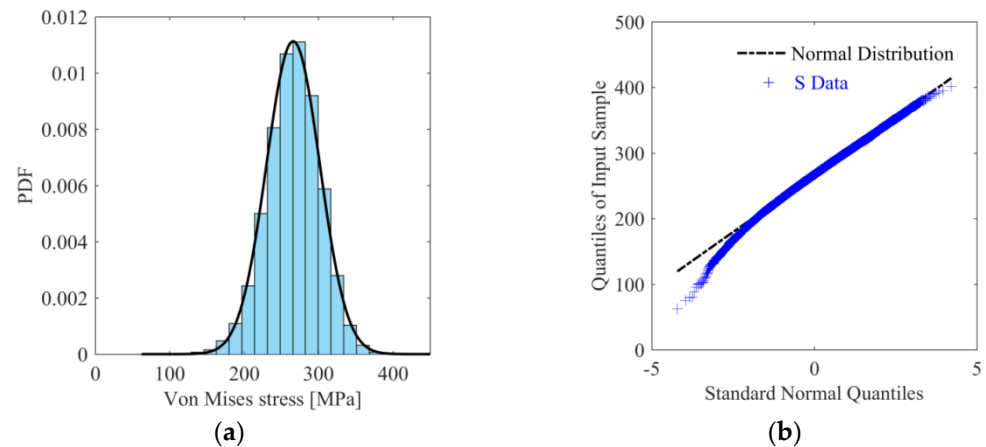


Figure 11. (a) Maximum equivalent stress (Von Mises stress) normalized histogram; (b) QQ plot out of the instances of S_2 .

Although the histogram in Figure 11a seems to be normal distributed, the point estimates of the maximum equivalent stress in the QQ plot in Figure 11b seem to deviate from the straight diagonal line. This is an indication that the set of data is not normally distributed. Therefore, Cornell’s reliability index cannot be utilized for the purpose of estimating the probability of failure.

5. Reliability Analysis of Curved Plates

This section lies within the proposed framework depicted in Figure 1, demonstrating the case for which there is not an analytical mathematical expression for the mapping

function $S(\cdot)$, that is, case study 3: a bow-defected plate subjected to hull-girder loads. In this case, a numerical procedure, such as the FEM, needs to be applied in order to obtain realizations of the response of the structure on the applied loads.

An FE model of the plate geometry with length a and width b , as shown in Figure 6, was generated. The problem has been cast in a linear static setting with the material being regarded as linear elastic and isotropic, since the applied loads were not expected to result in plastic deformation. In this context, a Young’s modulus of 200 GPa and a Poisson’s ratio of 0.3 were used as representative values of the shipbuilding steels. A clamped plate was considered for the study, and it was modeled using eight-node rectangular shell elements (SHELL281). Element size was determined by checking whether the maximum equivalent stress and the maximum deflection of the plate converged to a specific value. The mesh convergence study was made for alternative reasonably sized mesh options, and it was considered safe to assume that solution accuracy with respect to the mesh size has adequately converged by the 50 mm element edge case. The meshed plate is presented in Figure 12.

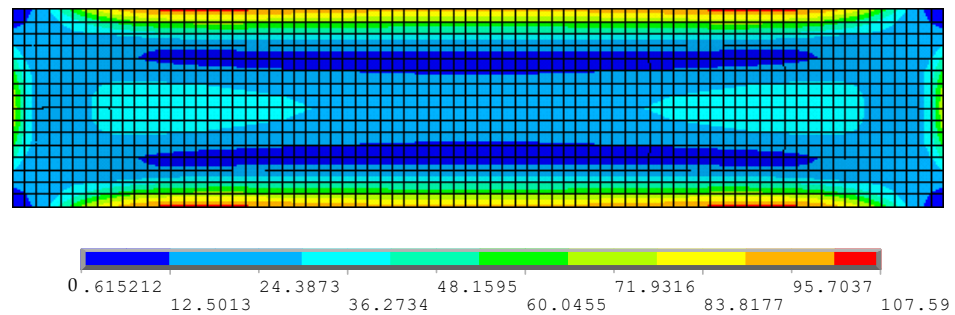


Figure 12. Clamped meshed plate—deformed and contour plot of the Von Mises stress component for an indicative pressure load realization and an indicative maximum initial deflection realization (aspect ratio $a/b = 4.725$).

It should be noted that for an indicative pressure load and indicative maximum initial deflection realizations, the structural displacement of the nodes of the clamped plate in the z direction seems to have the shape of camel humps in the longitudinal direction, as shown in Figure 13. This happened when the aspect ratio, a/b , was 4.725. However, when the plate was square, with an aspect ratio $a/b = 1$, the same structural displacement had the shape of one half-wave in the longitudinal direction and one half-wave in the transverse direction, as shown in Figures 13 and 14.

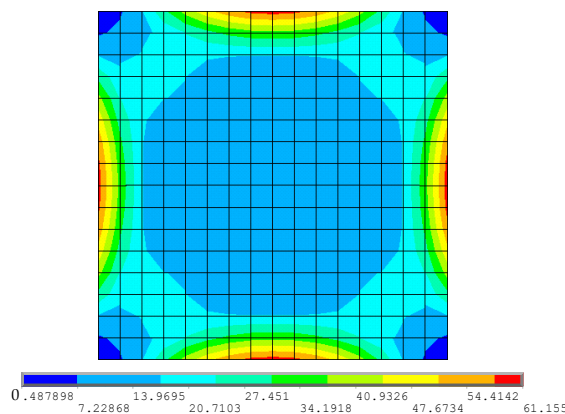


Figure 13. Clamped meshed plate—deformed and contour plot of the Von Mises stress component for an indicative pressure load realization and an indicative maximum initial deflection realization (aspect ratio $a/b = 1$).

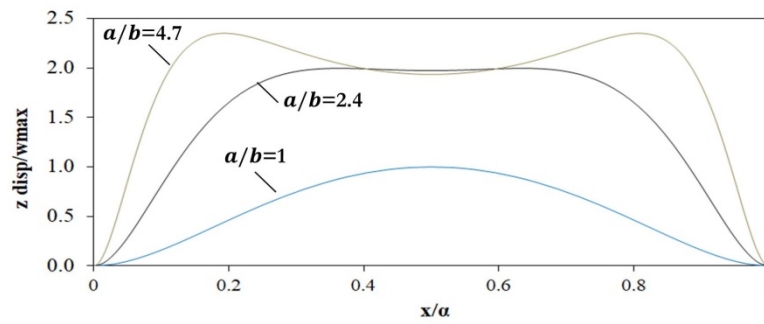


Figure 14. Shape of the structural displacement of the nodes of the plate in the z direction for various aspect ratios.

More specifically, it was noticed that when the aspect ratio took values higher than 2.3, the structural displacement of the nodes of the plate in the z direction was starting to take the shape of camel humps, which is obvious in the longitudinal direction. The above observation is also noticeable in Figure 14, where the shape of the structural displacement of the nodes of the plate in the z direction was plotted for various aspect ratios. The x axis corresponds to the x coordinate of the nodes over the total length, α , of the plate, and the y axis corresponds to the structural displacement of the nodes in the z direction over the maximum structural displacement of the plate with aspect ratio $\alpha/b = 1$.

However, as for the plates with an aspect ratio higher than 2.3, the irregular shape of the displacement of the nodes in the z direction (Figure 14) does not seem to contribute significantly to the final shape of the plate, as can be seen in Figure 15. Figure 15 depicts the final shape of the plate in the longitudinal direction for various aspect ratios.

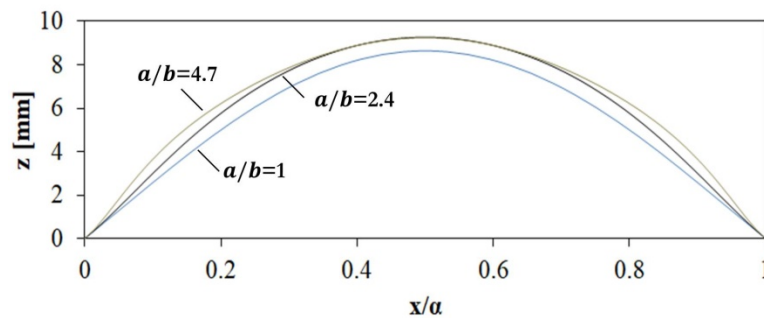


Figure 15. Final shape of the plate in the longitudinal direction for various aspect ratios.

The above observation is more obvious in Figure 16, where the initial shape, the structural displacement of the nodes of the plate in the z direction and the final shape of the plate were plotted along the length of a plate with an aspect ratio equal to 4.725.

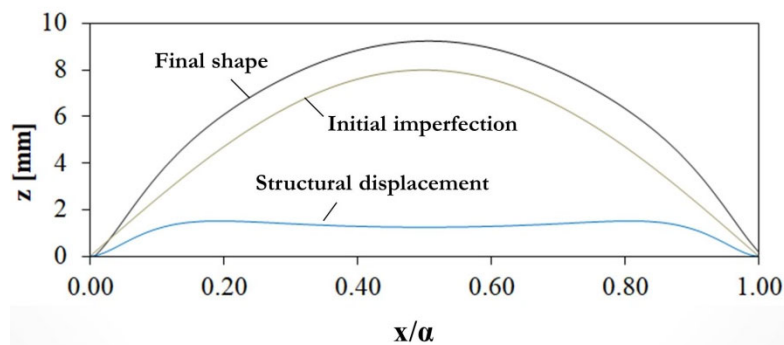


Figure 16. Shape of the initial imperfection, the structural displacement and the final shape of the plate.

Concerning the method that was utilized in order to estimate the probability of failure, there were two options, as indicated in Figure 1: the first option is to employ the MC simulation for the direct estimation of the probability of failure. In this case, a sample of size at least 1.4×10^{11} was needed to be generated from P_{sw} , and the FE model needed to be solved the same amount of times in order for the method to result in an indicative probability of failure, according to [34]. The size of these simulations was neither cost efficient nor achievable timewise. The second option is to employ the MC simulation for estimating the distribution of S and then solving the reliability problem analytically if the conditions allow. Following the latter path, the finite element model was repeatedly solved for 500 randomly sampled realizations of the load, P_{sw} , and of the maximum initial deflection, W_{max} , using the MC method.

After the FEA, the results of the maximum Von Mises stress (or S) were collected and statistically analyzed. As far as the distribution of the maximum Von Mises stress resulted from the FEA is concerned, a histogram and a Q-Q plot were constructed, as shown in Figure 17.

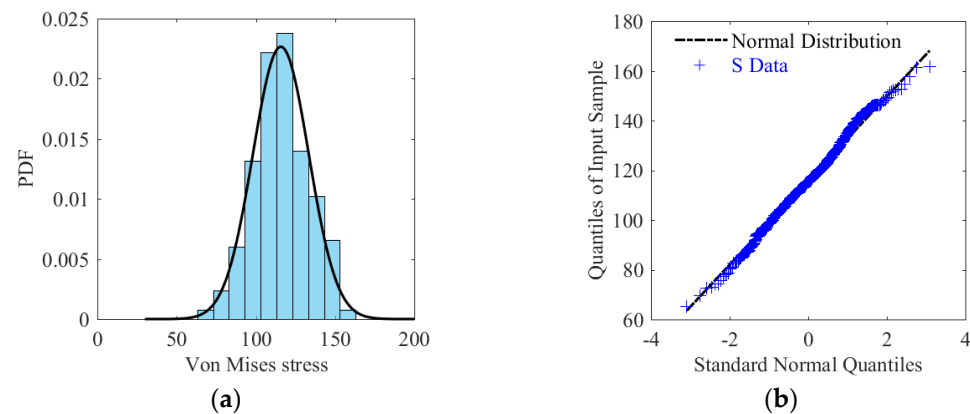


Figure 17. Clamped and initially deformed plate: (a) normalized histogram of the instances of S ; (b) QQ plot of the instances of S .

The plots shown in Figure 17 indicate that the values of the maximum Von Mises stress could come from a population which is normal distributed. Following the complete description of the statistical behavior of S , Cornell’s reliability index could be estimated according to Equation (6), resulting in a p_f equal to 6.30×10^{-11} , which was estimated according to Equation (11).

6. Discussion on Limitations of the Proposed Methods and Conclusions

In this work, a methodological framework for structural reliability assessment of marine structural elements is proposed. The fundamentals of structural reliability are briefly outlined, and the proposed SRA framework and its ingredients, i.e., the proposed methods for solving the reliability problem, are also detailed. The presented framework is demonstrated in a flat plate and a bow-defected one.

Having studied the literature body, it could be concluded that the MCS method for solving reliability problems is one of the most utilized methods when dealing with reliability problems. However, the large amount of sample data needed in order for the MC method to result in a more accurate solution, i.e., an indicative probability of failure, is usually neither cost efficient, concerning the computing resources, nor achievable timewise. That can be concluded after examining case study 1. One way to alleviate this computational burden and to improve the efficiency and accuracy of Monte Carlo estimation is to employ variance reduction techniques such as importance sampling [35–37]. In importance sampling, an alternate sampling density, i.e., importance sampling density (ISD) is chosen in order to sample realizations of the input random variables that greatly affect the estimate more frequently. This technique reduces the number of realizations required for an estimate while

introducing a bias on it, which is corrected by weighting the sample realizations. Therefore, a good choice of an ISD is of primary importance. Melchers [38] addressed the accuracy and efficiency of importance sampling and its application to series and parallel systems in structures. Generally, though, whenever computationally feasible, MCS is a robust method when sampling-based reliability methods are concerned, because its performance does not depend on the particular formulation of the limit-state function underlying the problem nor on the number of the input random variables.

Generally, another way to address the issues of accuracy and efficiency of the structural reliability assessment is to utilize surrogate models which replace the computationally expensive model with one that is much less expensive to evaluate, as seen in [39]. Various surrogate modeling approaches, such as polynomial response surface (PRS) [40,41], radial basis function (RBF), support vector machine (SVM) and Kriging [42], among others, have been adopted for reliability estimation [43]. In paper [44], the probability of failure was estimated utilizing a limit-state function that was approximated by a SVM-based radial basis function. The authors in [45] used the combination of response surface, FORM and importance sampling to perform reliability estimation.

The limitations of the analytical approach arose when examining more complicated problems, such as those in case study 2 and case study 3. Since most of the reliability problems deal with complex load effect functions and the random variable's distributions tend to be different, the analytical approach seems to be rarely applicable to the reliability problems. Additionally, MVFOSM methods have two basic shortcomings. Firstly, the limit-state function is linearized at the mean value of basic variables, and when it is nonlinear, significant errors may be introduced at increasing distances from the linearizing point by neglecting higher-order terms in Taylor's series expansion. Secondly, since the linear expansions are taken about the mean value point, the method fails to be invariant to different mechanically equivalent formulations of the same problem.

Finally, the present study showed that when dealing with a more practical and realistic problem, such as the one in case study 3, then a numerical procedure, such as FEM, needs to be applied in order to proceed to the solution. In fact, if no explicit expression exists for the load effect function, then the analytical method and the MVFOSM method are no longer applicable. Following the FEA, the utilization of the MC method, either for a direct estimation of the probability of failure or for the estimation of the distribution of the load effect, is unavoidable. The latter method, though, is not always applicable, since certain conditions must be met.

Author Contributions: Conceptualization, K.A.; methodology, K.A. and V.M.; formal analysis, K.A. and V.M.; investigation, K.A. and V.M.; data curation, V.M. writing—original draft preparation, V.M.; writing—review and editing, K.A.; visualization, V.M.; supervision, K.A.; project administration, K.A. All authors have read and agreed to the published version of the manuscript.

Funding: This research received no external funding.

Institutional Review Board Statement: Not applicable.

Informed Consent Statement: Not applicable.

Data Availability Statement: Not applicable.

Conflicts of Interest: The authors declare no conflict of interest.

Appendix A

As far as the mapping function S , that is considered to be a linear function of the basic variables (\mathbf{X}), is concerned, its formulation is as follows:

$$S = \alpha_0 + \sum_{i=1}^n \alpha_i X_i \quad (\text{A1})$$

Taking into account that the basic random variables are taken to be normal distributed, the mean and the standard deviation of the variable S can be defined as

$$\mu_S = \alpha_0 + \sum_{i=1}^n \alpha_i \mu_i \tag{A2}$$

$$\sigma_S^2 = \sum_{i=1}^n \alpha_i^2 \sigma_{X_i}^2 + 2 \sum_{i=1}^n \sum_{j=i+1}^n \rho_{ij} \alpha_i \alpha_j \sigma_i \sigma_j \tag{A3}$$

where α_0 and α_i are constants and ρ_{ij} is the correlation coefficient between X_i and X_j and $\mu_i = \mu_{X_i}$ and $\sigma_i = \sigma_{X_i}$. According to Equation (5), the mean value and the standard deviation of G are:

$$\mu_G = \mu_R - \mu_S \tag{A4}$$

$$\sigma_G = \sqrt{\sigma_R^2 + \sigma_S^2 + 2\rho_{R,S}\sigma_R\sigma_S} \tag{A5}$$

where $\rho_{R,S}$ is the correlation coefficient between R and S .

Concerning the case in which the basic variables are lognormal and independent, then the logarithm of S , i.e., $\ln S$, is normal distributed, since the sum of the logarithms of the random variables is normal distributed. The mean and the standard deviation of the variable $\ln S$ can be defined as

$$\mu_{\ln S} = b_0 + \sum_{i=1}^n b_i \mu_i' \tag{A6}$$

$$\sigma_{\ln S}^2 = \sum_{i=1}^n b_i^2 \sigma_{X_i}'^2 + 2 \sum_{i=1}^n \sum_{j=i+1}^n \rho_{ij}' b_i b_j \sigma_i' \sigma_j' \tag{A7}$$

where b_0 and b_i are constants and ρ_{ij}' is the correlation coefficient between $\ln X_i$ and $\ln X_j$ and $\mu_i' = \mu_{\ln X_i}$ and $\sigma_i' = \sigma_{\ln X_i}$.

If S is a non-linear function of the basic random variables X_i , the approximate mean and variance of S are obtained by using Taylor's series expansion and truncating the series to the required approximation. If

$$S = f(X_1, X_2, \dots, X_n) \tag{A8}$$

the first-order approximations of the mean and the variance S are given by

$$\mu_S \approx f(\mu_1, \mu_2, \dots, \mu_n) \tag{A9}$$

$$\sigma_S^2 \approx \sum_{i=1}^n \sum_{j=1}^n \left[\left. \frac{\partial f}{\partial X_i} \right|_{\mu} \right] \left[\left. \frac{\partial f}{\partial X_j} \right|_{\mu} \right] \rho_{ij} \tag{A10}$$

$\left[\left. \frac{\partial f}{\partial X_i} \right|_{\mu} \right]$ means that the derivative is evaluated at the mean values of the variables. If X_i is uncorrelated, then

$$\sigma_S^2 \approx \sum_{i=1}^n \left[\left. \frac{\partial f}{\partial X_i} \right|_{\mu} \right]^2 \sigma_{X_i}^2 \tag{A11}$$

Figure 9 illustrates the transformation of the density function $f_S(s)$ according to the relation $s = f(x)$ and the linear approximation of the relation between the two random variables.

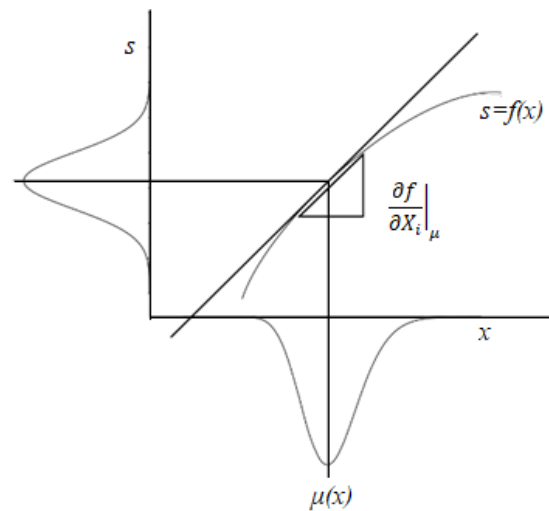


Figure A1. The transformation of the density function $f_S(s)$ according to the relation $s = f(x)$ and the linear approximation of the relation between the two random variables.

References

- Ivanov, L.D.; Chen, N.-Z. On the presentation of ship's hull girder section modulus in probabilistic formats. *Ships Offshore Struct.* **2017**, *12*, 1024–1036. [CrossRef]
- Ivanov, L.D. Reliability estimation of ship's hull girder in probabilistic terms when ultimate strength is used as a failure mode. *Ships Offshore Struct.* **2013**, *8*, 141–153. [CrossRef]
- Vasileiou, A.S.; Anyfantis, K.N. Reliability analysis of SHS compression members in shipbuilding: Derivation of probabilistic buckling curves. *Ships Offshore Struct.* **2023**, *18*, 338–348. [CrossRef]
- Georgiadis, D.G.; Samuelides, M.S. Stochastic geometric imperfections of plate elements and their impact on the probabilistic ultimate strength assessment of plates and hull-girders. *Mar. Struct.* **2021**, *76*, 102920. [CrossRef]
- IACS. Common Structural Rules for Double Hull Oil Tankers. Available online: <https://iacs.org.uk/resolutions/common-structural-rules/csr-for-bulk-carriers-and-oil-tankers> (accessed on 24 October 2023).
- Teixeira, A.; Soares, C.G. Assessment of partial safety factors for tankers. In *JCSS Workshop on Reliability Based Code Calibration*; JCSS: Zurich, Switzerland, 2002; pp. 1–15.
- Assakkaf, I.A.; Ayyub, B.M.; Hess, P.E.; Atua, K. Reliability-Based Load and Resistance Factor Design (LRFD) Guidelines for Stiffened Panels and Grillages of Ship Structures. *Nav. Eng. J.* **2002**, *114*, 89–112. [CrossRef]
- Anyfantis, K.N.; Pantazopoulou, S.; Papanikolaou, N. Generalized probabilistic response surfaces for the buckling strength assessment of stiffened panels. *Thin-Walled Struct.* **2023**, *189*, 110860. [CrossRef]
- Assakkaf, I.A.; Ayyub, B.M. Reliability-based design of unstiffened panels for ship structures. In *Proceedings of the 3rd International Symposium on Uncertainty Modeling and Analysis and Annual Conference of the North American Fuzzy Information Processing Society*, College Park, MA, USA, 17–20 September 1995; pp. 692–697.
- Karras, S.I.; Anyfantis, K.N. Probabilistic modelling of the buckling strength of steel plates in ship hulls. In *Proceedings of the 6th International Conference on Maritime Technology and Engineering*, Lisbon, Portugal, 22–24 May 2022.
- Elhanafi, A.S.; Leheta, H.W.; Badran, S.F. Time-variant reliability analysis of novel deck and bottom panels. *Ocean Eng.* **2017**, *133*, 73–88. [CrossRef]
- Parunov, J.; Senjanović, I.; Soares, C.G. Hull-girder reliability of new generation oil tankers. *Mar. Struct.* **2007**, *20*, 49–70. [CrossRef]
- Soares, C.G.; Teixeira, A. Structural reliability of two bulk carrier designs. *Mar. Struct.* **2000**, *13*, 107–128. [CrossRef]
- Mansour, A.E. Probabilistic Design Concepts in Ship Structural Safety and Reliability. *Trans. SNAME* **1993**, *80*, 64–97.
- Fang, C.; Das, P.K. Survivability and reliability of damaged ships after collision and grounding. *Ocean Eng.* **2005**, *32*, 293–307. [CrossRef]
- Bužančić Primorac, B.; Parunov, J.; Guedes Soares, C. Structural reliability analysis of ship hulls accounting for collision or grounding damage. *J. Mar. Sci. Appl.* **2020**, *19*, 717–733. [CrossRef]
- Gaspar, B.; Soares, C.G. Hull girder reliability using a Monte Carlo based simulation method. *Probabilistic Eng. Mech.* **2013**, *31*, 65–75. [CrossRef]
- Piscopo, V.; Scamardella, A. Sensitivity analysis of hull girder reliability in intact condition based on different load combination methods. *Mar. Struct.* **2019**, *64*, 18–34. [CrossRef]
- Casella, G.; Dogliani, M.; Soares, C.G. Reliability-based design of the primary structure of oil tankers. *Oceanogr. Lit. Rev.* **1998**, *4*, 707. [CrossRef]

20. Class, N.K. Investigation Report on Structural Safety of Large Container Ships. *Tokyo Cl. NK*. 2014. Available online: https://www.classnk.or.jp/hp/pdf/news/Investigation_Report_on_Structural_Safety_of_Large_Container_Ships_EN_ClassNK.pdf (accessed on 24 October 2023).
21. Hussein, A.; Soares, C.G. Reliability and residual strength of double hull tankers designed according to the new IACS common structural rules. *Ocean Eng.* **2009**, *36*, 1446–1459. [[CrossRef](#)]
22. Guia, J.; Teixeira, A.; Soares, C.G. Probabilistic modelling of the hull girder target safety level of tankers. *Mar. Struct.* **2018**, *61*, 119–141. [[CrossRef](#)]
23. Campanile, A.; Piscopo, V.; Scamardella, A. Conditional reliability of bulk carriers damaged by ship collisions. *Mar. Struct.* **2018**, *58*, 321–341. [[CrossRef](#)]
24. Ranganathan, R. *Structural Reliability Analysis and Design*; Jaico Publishing House: Mumbai, India, 1999.
25. Faber, M.H. *Statistics and Probability Theory: In Pursuit of Engineering Decision Support*; Springer Science & Business Media: Berlin, Germany, 2012; Volume 18.
26. Yao, T.; Fujikubo, M. *Buckling and Ultimate Strength of Ship and Ship-Like Floating Structures*; Butterworth-Heinemann: Oxford, UK, 2016.
27. Li, S.; Benson, S. A probabilistic approach to assess the computational uncertainty of ultimate strength of hull girders. *Reliab. Eng. Syst. Saf.* **2021**, *213*, 107688. [[CrossRef](#)]
28. Georgiadis, D.G.; Samuelides, E.S.; Straub, D. A Bayesian analysis for the quantification of strength model uncertainty factor of ship structures in ultimate limit state. *Mar. Struct.* **2023**, *92*, 103495. [[CrossRef](#)]
29. Xu, M.C.; Teixeira, A.; Soares, C.G. Reliability assessment of a tanker using the model correction factor method based on the IACS-CSR requirement for hull girder ultimate strength. *Probabilistic Eng. Mech.* **2015**, *42*, 42–53. [[CrossRef](#)]
30. Chen, X.; Shen, S. Uncertainties in material strength geometric and load variables. *J. Build. Struct.* **1992**, *13*, 11–18.
31. Teixeira, A.; Guedes Soares, C. *Reliability Assessment of Plate Elements with Random Properties*; Taylor & Francis Group: London, UK, 2011; pp. 1361–1375.
32. Hanif, M.I.; Adiputra, R.; Prabowo, A.R.; Yamada, Y.; Firdaus, N. Assessment of the ultimate strength of stiffened panels of ships considering uncertainties in geometrical aspects: Finite element approach and simplified formula. *Ocean Eng.* **2023**, *286*, 115522. [[CrossRef](#)]
33. Li, S.; Georgiadis, D.G.; Samuelides, M.S. A comparison of geometric imperfection models for collapse analysis of ship-type stiffened plated grillages. *Eng. Struct.* **2022**, *250*, 113480. [[CrossRef](#)]
34. Melchers, R.E.; Beck, A.T. *Structural Reliability Analysis and Prediction*; John Wiley & Sons: Hoboken, NJ, USA, 2018.
35. Pannerselvam, K.; Yadav, D.; Ramu, P. Scarce Sample-Based Reliability Estimation and Optimization Using Importance Sampling. *Math. Comput. Appl.* **2022**, *27*, 99. [[CrossRef](#)]
36. Melchers, R. Search-based importance sampling. *Struct. Saf.* **1990**, *9*, 117–128. [[CrossRef](#)]
37. Qu, X.; Haftka, R. Reliability-based design optimization using probabilistic sufficiency factor. *Struct. Multidiscip. Optim.* **2004**, *27*, 314–325. [[CrossRef](#)]
38. Melchers, R. Importance sampling in structural systems. *Struct. Saf.* **1989**, *6*, 3–10. [[CrossRef](#)]
39. Bichon, B.J.; McFarland, J.M.; Mahadevan, S. Efficient surrogate models for reliability analysis of systems with multiple failure modes. *Reliab. Eng. Syst. Saf.* **2011**, *96*, 1386–1395. [[CrossRef](#)]
40. Goswami, S.; Ghosh, S.; Chakraborty, S. Reliability analysis of structures by iterative improved response surface method. *Struct. Saf.* **2016**, *60*, 56–66. [[CrossRef](#)]
41. Gavin, H.P.; Yau, S.C. High-order limit state functions in the response surface method for structural reliability analysis. *Struct. Saf.* **2008**, *30*, 162–179. [[CrossRef](#)]
42. Gaspar, B.; Teixeira, A.P.; Soares, C.G. Assessment of the efficiency of Kriging surrogate models for structural reliability analysis. *Probabilistic Eng. Mech.* **2014**, *37*, 24–34. [[CrossRef](#)]
43. Chatterjee, T.; Chakraborty, S.; Chowdhury, R. A critical review of surrogate assisted robust design optimization. *Arch. Comput. Methods Eng.* **2019**, *26*, 245–274. [[CrossRef](#)]
44. Dai, H.-Z.; Zhao, W.; Wang, W.; Cao, Z. An improved radial basis function network for structural reliability analysis. *J. Mech. Sci. Technol.* **2011**, *25*, 2151–2159. [[CrossRef](#)]
45. Foschi, R.; Li, H.; Zhang, J. Reliability and performance-based design: A computational approach and applications. *Struct. Saf.* **2002**, *24*, 205–218. [[CrossRef](#)]

Disclaimer/Publisher’s Note: The statements, opinions and data contained in all publications are solely those of the individual author(s) and contributor(s) and not of MDPI and/or the editor(s). MDPI and/or the editor(s) disclaim responsibility for any injury to people or property resulting from any ideas, methods, instructions or products referred to in the content.